Dynamical structure factor $S(q,\omega)$ of liquid helium II at zero temperature

W. Götze and M. Lücke*
Physik-Department der Technischen Universität and Max-Planck-Institut für Physik, München, Germany
(Received 6 October 1975)

The dynamical density correlation function of liquid helium II at zero temperature is expressed in terms of a static restoring force Ω_0 and a polarization operator M within Mori's theory. M is approximated in terms of two-mode decay integrals and Ω_0 is related self-consistently to the liquid structure factor. The nonlinear integral equations for M and Ω_0 are solved by an iteration procedure and the dynamical structure factor $S(q,\omega)$ obtained is compared with the experimental results of Cowley and Woods. The elementary excitation spectrum calculated has a roton minimum Δ of 11 °K and shows Pitaevskij bending for large momenta. The existence of a resonance of $S(q,\omega)$ is found to be the explanation for the measured excitation peak to exceed 2Δ. The variation of the single excitation strength as a function of momentum is analyzed. The multiphonon contribution to $S(q,\omega)$ is discussed and the existence of a double-peak structure therein is found for intermediate wave numbers.

I. INTRODUCTION

Since Landau[1] introduced the concept of an elementary excitation to provide a microscopic theory for the two-fluid hydrodynamics of liquid helium II much effort has been invested to working out a first-principles derivation of his phonon-roton spectrum. Bogoliubov[2] studied the model of a weakly interacting Bose gas; he was able to derive for his model the elementary excitation picture as a consequence of the Bose condensation. The excitation spectrum exhibited as low-lying-states phonons only: a result necessary to explain superfluidity. The model was extended later[3] to a theory of dilute Bose systems with essentially realistic interactions. The Bogoliubov model and its extensions do not yield a theory of rotons. Feynman[4] could explain the rotons as a result of the high density of helium. He showed that Bijl's[5] suggestion for an excitation state

$$\psi_{\vec{q}}^{0} = \rho_{\vec{q}}\psi \tag{1a}$$

is a reasonable test function, because of the interplay of Bose statistics and strong interaction at high density. Here ψ is the ground-state wave function and $\rho_{\vec{q}}$ denotes the density operator of wave number $\vec{q}$. Calculating the expectation value of the Hamiltonian with $\psi_{\vec{q}}^{0}$, one gets[4,5] as an upper bound for the excitation energy

$$\epsilon_0(q) = q^2/2ms(q). \tag{1b}$$

Here m denotes the helium mass and $s(q)$ is the structure factor. Every liquid, contrary to the dilute systems of the Bogoliubov model, exhibits a peak in $s(q)$ for q roughly equal to the reciprocal interparticle distance. This peak then implies a roton minimum for $q \simeq 2$ Å^{-1}, in agreement with Landau's[1] prediction.

The minimal roton energy Δ according to the Bijl-Feynman spectrum (1b) is larger than the experimental one by a factor of 2. The main reason for this deficiency has been found by Feynman and Brenig.[6] The continuity equation forces the roton wave packet to be surrounded by a back flow of liquid. Estimating this back flow on the basis of classical hydrodynamics they found that, essentially, m in Eq. (1a) has to be replaced by $m^* = \frac{3}{2}m$. A detailed calculation of the excitation spectrum with a trial wave function incorporating back flow was carried out by Feynman and Cohen.[7] For Δ they obtained 11.9 °K.

Within Beliaev's[3] field-theoretical formulation of the helium problem, the decay of one elementary excitation into two was analyzed by Pitaevskij.[8] He carried out an asymptotic expansion of the scattering amplitudes and self-energies near the decay thresholds. In particular he found that the excitation spectrum cannot exceed 2Δ. The spectrum has to bend and approaches 2Δ with zero group velocity. The Feynman-Cohen spectrum is not in agreement with the Pitaevskij result.

Condidering the Bijl-Feynman wave functions (1a) as the zeroth approximation, Kuper[9] calculated the first perturbation correction to Δ taking double density fluctuations as the most important intermediate states into account. Jackson and Feenberg[10,11] have carried out the calculation of $\epsilon_1(q)$ for all momenta and obtained a spectrum resembling the one of Feynman and Cohen. Jackson[11] also presented a calculation of the complete dynamical structure factor $S(q,\omega)$. In a first-order calculation one uses the zeroth-order frequencies (1b) as energies for the decaying quasiparticles. These energies $\epsilon_0(q)$ are very different from $\epsilon_1(q)$, and this inconsistency is the reason for not getting a correct Pitaevskij bending. Jackson[11] proposed

a consistent theory such that their original result[10] is obtained as a first approximation; the result[12] $\epsilon(q)$ of this theory, being lower than $\epsilon_1(q)$, is not satisfactory, however.

A very helpful qualitative discussion of the dynamical structure factor $S(q,\omega)$ was given by Miller, Pines, and Nozières.[13] They realized that the Feynman-Cohen wave function has the form

$$\psi_{\vec{q}}^{\frac{1}{2}} = \left(\rho_{\vec{q}} + \sum_{\vec{p}} A(\vec{q},\vec{p})\rho_{\vec{p}}\rho_{\vec{q}-\vec{p}}\right)\psi, \tag{2}$$

thus being a superposition of single and double density excitations. Hence they concluded that the back flow is approximately identical to taking into account the virtual two-roton excitations. One should expect a kind of optical potential for the rotons whose imaginary part describes the roton decay at large energies and whose real part renormalizes the excitation frequencies at low energies. The real part should also be responsible for the characteristic variation of the resonance intensity as a function of wave number.

It should be mentioned that a first-principles calculation of the excitation spectrum has also been carried out by Brueckner and Sawada.[14] The result is similar to the one by Feynman and Cohen[7] but the theory was rejected because of internal inconsistencies.[15] Attempts[16] have been published to modify Bogoliubov's results[2] in order to get a roton spectrum with wave function (2). The results disagree with the Pitaevskij[8] theorems and show also other deficiencies.[17]

An interesting consequence of the Pitaevskij singularities has been realized by Ruvalds and Zawadowski.[18] If the effective interaction for the scattering of two rotons is attractive, there will be a two-roton bound state below 2Δ. They worked out the modifications of $S(q,\omega)$ due to such a bound state within a simplified model. Apparently the modifications of $S(q,\omega)$ are so small that the neutron scattering data are not influenced within the resolution available at present. For this reason we will ignore the two-roton scattering in the following. The present theory does not add anything to the previous discussions[19] of the excitation anomalies in the sound-wave region and so this point will not be touched either.

The excitation spectrum of helium has been measured by inelastic neutron scattering experiments.[20] The neutron scattering cross section for momentum transfer q and energy loss ω is proportional to the dynamical structure factor $S(q,\omega)$ and so this quantity has been determined[21] for a large area of the q-ω plane. In this paper we want to present a theory for $S(q,\omega)$ which allows for a mathematical formulation of Miller *et al.*'s arguments. Equations will be derived allowing one to combine the back-flow phenomenon with Pitaevskij's scattering singularities. The solution for $S(q,\omega)$ obtained within this theory is in better agreement with experiment than the results achieved previously.

In Sec. II the formal scheme for the correlation functions is given within Mori's theory.[22] Then the basic approximations are formulated and the closed nonlinear equations for $S(q,\omega)$ are derived (Sec. III.). In Sec. IV a modified iteration scheme is studied and a consistent solution is obtained. In Sec. V the results of the present theory are compared with the experiment.

II. FORMALISM

A. Correlation functions

As usual[23] we introduce the A-B dynamical susceptibility

$$\chi_{AB}(z) = -\langle\langle A^*; B\rangle\rangle_z, \tag{3}$$

where the Zubarev function is defined as the Laplace transform of $-i\langle[A^*(t),B]\rangle$. $\chi(z)$, like all functions analytic off the real axis and decaying for large z fast enough, can be written as spectral integrals:

$$F(z) = \frac{1}{\pi}\int d\omega \frac{F''(\omega)}{\omega - z}, \tag{4a}$$

$$F(\omega \pm i0) = F'(\omega) \pm iF''(\omega). \tag{4b}$$

In particular

$$\chi''_{AB}(\omega) = \frac{1}{2}\int dt\, e^{i\omega t}\langle[A^*(t),B]\rangle. \tag{5a}$$

The fluctuation-dissipation theorem reads in the present notation

$$\langle A^*(t)B\rangle = \frac{1}{\pi}\int d\omega\, e^{-i\omega t}[1+n(\omega)]\chi''_{AB}(\omega), \tag{5b}$$

where $n(\omega) = 1/(e^{\omega/T}-1)$ is the Bose distribution function at temperature T. If $\rho_{\vec{q}}$ denotes the density fluctuation operator for wave number $\vec{q}$, the dynamical structure factor $S(q,\omega)$, depending on modulus q only, is given[24] as the Fourier transform of $\langle\rho^*_{\vec{q}}(t)\rho_{\vec{q}}\rangle$, and, hence,

$$S(q,\omega) = 2[1+n(\omega)]\chi''(q,\omega), \tag{6}$$

where $\chi(q,z) = -\langle\langle\rho^*_{\vec{q}};\rho_{\vec{q}}\rangle\rangle_z$ is the density-density correlation function.

It is convenient to introduce also the Kubo function $\phi(q,z)$ related to the susceptibility by

$$\phi(q,z) = [\chi(q,z) - \chi_0(q)]/z, \tag{7a}$$

$$\phi''(q,\omega) = \chi''(q,\omega)/\omega. \tag{7b}$$

Here $\chi_0(q) = \chi(q,z=0)$ is the static density-density

response. Introducing the scalar product $(A|B) = \chi_{AB}(z=0)$ in the linear space of dynamical variables, $\phi_{AB}(z)$ is the Laplace transform of $(A(t)|B)$. With the Liouville operator $\mathfrak{L}$ defined by $\mathfrak{L}A = [H,A]$ one can represent then the Kubo function as a resolvent matrix element,

$$\phi(q,z) = (\rho_{\vec{q}}|(\mathfrak{L}-z)^{-1}|\rho_{\vec{q}}). \tag{8}$$

As usual one verifies

$$\phi''(q,\omega) = \phi''(q,-\omega) = \phi''(q,\omega)^* \geq 0. \tag{9}$$

From Eq. (8) one gets the asymptotic expansion

$$\phi(q,z) = -[\chi_0(q)/z][1+\Omega_0^2(q)/z^2 + O(1/z^4)], \tag{10}$$

where $\chi_0(q)\Omega_0^2(q) = (\rho_q|\mathfrak{L}^2|\rho_q)$. Using the general relation

$$(A|\mathfrak{L}|B) = \langle [A^*,B]\rangle, \tag{11}$$

the continuity equation $\mathfrak{L}\rho_{\vec{q}} = -q_\alpha j_\alpha(\vec{q})$, where $j_\alpha(\vec{q})$ denotes the current operator, and the known commutation relation

$$[j_\alpha^*(\vec{q}),\rho_{\vec{p}}] = -(p_\alpha/m)\rho_{\vec{p}-\vec{q}}, \tag{12}$$

one finds

$$(\rho_{\vec{q}}|\mathfrak{L}^2|\rho_{\vec{q}}) = q^2/m. \tag{13a}$$

Therefore, the characteristic frequency $\Omega_0(q)$ is given by

$$\Omega_0^2(q) = q^2/m\chi_0(q). \tag{13b}$$

Expansion (10) due to Eq. (4a) is equivalent to the sum rules

$$\frac{1}{\pi}\int_0^\infty d\omega\, \omega^{-1}\chi''(q,\omega) = \tfrac{1}{2}\chi_0(q), \tag{14}$$

$$\frac{1}{\pi}\int_0^\infty d\omega\, \omega\chi''(q,\omega) = \frac{1}{2m}q^2. \tag{15}$$

Equation (14) is the static sum rule for χ'' and Eq. (15) represents the f-sum rule. Furthermore, one obtains from Eq. (5b) the expression for the structure factor $s(q) = \langle \rho_{\vec{q}}^* \rho_{\vec{q}}\rangle$:

$$\frac{1}{\pi}\int_0^\infty d\omega\, \coth\left(\frac{\omega}{2T}\right)\chi''(q,\omega) = s(q). \tag{16}$$

B. Polarization operator

To introduce some effective potential for the propagation of density modes, which are described as resonances of $\phi(q,z)$, we use Mori's[22] theory. Denoting with $\mathcal{P}$ the projector on $\rho_{\vec{q}}$

$$\mathcal{P} = |\rho_{\vec{q}})\chi_0(q)^{-1}(\rho_{\vec{q}}| \tag{17}$$

and with $\mathcal{Q}$ its orthogonal complement one can write

$$\mathcal{P}(\mathfrak{L}-z)^{-1}\mathcal{P} = \mathcal{P}[\mathcal{P}\mathfrak{L}\mathcal{P} - z + \mathcal{P}\mathfrak{L}\mathcal{Q}(\mathcal{Q}\mathfrak{L}\mathcal{Q} - z\mathcal{Q})^{-1}\mathcal{Q}\mathfrak{L}\mathcal{P}]^{-1}\mathcal{P}. \tag{18}$$

Taking the $\rho_{\vec{q}} - \rho_{\vec{q}}$ matrix element one gets

$$\phi(q,z) = \frac{\chi_0(q)}{m(q,z)/\chi_0(q) - z}, \tag{19a}$$

where

$$m(q,z) = -(\mathcal{Q}\mathfrak{L}\rho_{\vec{q}}|(\mathcal{Q}\mathfrak{L}\mathcal{Q}-z)^{-1}|\mathcal{Q}\mathfrak{L}\rho_{\vec{q}}) \tag{19b}$$

is another resolvent matrix element. Since $\rho_{\vec{q}}$ is orthogonal to $\mathfrak{L}\rho_{\vec{q}}$ one gets $\mathcal{Q}\mathfrak{L}\rho_{\vec{q}} = \mathfrak{L}\rho_{\vec{q}}$. Repetition of the preceding procedure yields

$$m(q,z) = \frac{-\chi_1(q)}{M(q,z)+z}, \tag{19c}$$

with $\chi_1(q) = (\mathfrak{L}\rho_{\vec{q}}|\mathfrak{L}\rho_{\vec{q}}) = q^2/m$, and

$$M(q,z)\chi_1(q) = (\mathcal{Q}'\mathcal{Q}\mathfrak{L}\mathcal{Q}\mathfrak{L}\rho_{\vec{q}}|(\mathcal{Q}'\mathcal{Q}\mathfrak{L}\mathcal{Q}\mathcal{Q}'-z)^{-1}|\mathcal{Q}'\mathcal{Q}\mathfrak{L}\mathcal{Q}\mathfrak{L}\rho_{\vec{q}}). \tag{19d}$$

Here $\mathcal{Q}'$ is the projector perpendicular to $\mathfrak{L}\rho_{\vec{q}}$. One verifies

$$\mathcal{Q}'\mathcal{Q}\mathfrak{L}\mathcal{Q}\mathcal{Q}' = \mathcal{Q}'\mathfrak{L}\mathcal{Q}' \tag{20a}$$

and

$$\mathcal{Q}'\mathcal{Q}\mathfrak{L}\mathcal{Q}\mathfrak{L}\rho_{\vec{q}} = \mathcal{Q}\mathfrak{L}^2\rho_{\vec{q}}. \tag{20b}$$

Summarizing the preceding formulas and Eqs. (7a) and (13) one arrives at the following expression for the susceptibility

$$\chi(q,z) = \frac{-q^2/m}{z^2 - \Omega_0(q)^2 + zM(q,z)}. \tag{21}$$

The correlation function is represented in terms of a polarization operator $M(q,z)$:

$$M(q,z) = (\tau_{\vec{q}}|(\mathcal{Q}'\mathfrak{L}\mathcal{Q}'-z)^{-1}|\tau_{\vec{q}}). \tag{22}$$

$M(q,z)$ is the correlation of the incoherent fluctuating force

$$\tau_{\vec{q}} = \mathcal{Q}\mathfrak{L}^2\rho_{\vec{q}} = \mathfrak{L}^2\rho_{\vec{q}} - \Omega_0(q)^2\rho_{\vec{q}} \tag{23}$$

whose time evolution is restricted to a space perpendicular to $\rho_{\vec{q}}$ and $\mathfrak{L}\rho_{\vec{q}}$. Since the one phonon resonances are projected out in M, this quantity can be expected to vary smoothly. Hence M is a good candidate for approximations.

C. Elementary excitations

Later we will see that there are elementary excitations in agreement with Landau's[1] reasoning: $\chi''(q,\omega)$ has a sharp resonance for $\omega = \epsilon(q)$, and there are no excitations below $\epsilon(q)$. This means

$$\epsilon(q)^2 - \Omega_0(q)^2 = -\epsilon(q)M'(q,\epsilon(q)) \tag{24}$$

and

$$M''(q,\omega) = 0 \quad \text{for } |\omega| \leq \epsilon(q). \tag{25}$$

The preceding equations determine the elementary excitation spectrum. $M''(q,\omega)$ is even in ω and so one gets from Eq. (4) the Kramers-Kronig relation

$$M'(q,\omega)=\frac{2\omega}{\pi}P\int_0^\infty \frac{M''(q,\epsilon)}{\epsilon^2-\omega^2}d\epsilon. \tag{26}$$

Since M'' is positive, Eq. (25) implies that $M'(q,\omega)$ is positive and increasing with ω for $0<\omega<\epsilon(q)$. Hence $\epsilon(q)<\Omega_0(q)$. Expanding the denominator of Eq. (21) around $\epsilon(q)$ one gets

$$\chi''(q,\omega)=Z(q)\pi\delta(\omega-\epsilon(q))+\chi_c''(q,\omega). \tag{27}$$

Here χ_c'' describes the smooth continuous part of the susceptibility due to $M''(q,\omega)\neq 0$; $Z(q)$ is the intensity of the one excitation peak in the scattering cross section. Introducing the relative strength factor

$$f(q)=Z(q)/s(q), \tag{28a}$$

one finds

$$f(q)=\frac{\epsilon_0(q)}{\epsilon(q)}\left(\frac{1}{2}+\frac{1}{2}\frac{\Omega_0^2(q)}{\epsilon^2(q)}+\frac{1}{2}\frac{\partial M'(q,\epsilon(q))}{\partial\omega}\right)^{-1}. \tag{28b}$$

At zero temperature the sum rule (16) implies

$$1-f(q)=\frac{1}{\pi}\int_0^\infty d\omega\frac{\chi_c''(q,\omega)}{s(q)}. \tag{29}$$

The preceding formulas and discussions are exact. The problem consists of calculating $M''(q,\omega)$. In the simplest approximation $M''\simeq 0$ one gets $\chi_c''(q,\omega)\simeq 0$. Then the sum rules fix the dynamical susceptibility[13]:

$$f(q)\simeq 1, \tag{30a}$$

$$\chi_0(q)\simeq 2s(q)/\epsilon(q), \tag{30b}$$

$$\epsilon(q)\simeq\Omega_0(q), \tag{30c}$$

and $\epsilon(q)$ is the Bijl-Feynman value (1b).

III. TWO-MODE APPROXIMATION

A. Two-mode propagation

The space in which $\tau(\vec{q})$ moves under action of $\mathcal{Q}'\mathcal{L}\mathcal{Q}'$ can be imagined as spanned by a complete set of operators of even parity under time reversal. The simplest of such vectors are the two density fluctuation modes $\rho_{\vec{k}_1}\rho_{\vec{k}_2}$. The latter operators create those parts of the wave function (2) used in the Feynman and Cohen description of the backflow. The simplest reasonable approximation thus consists of neglecting all other vectors by writing

$$(\mathcal{Q}'\mathcal{L}\mathcal{Q}'-z)^{-1}\simeq\mathcal{P}_2(\mathcal{Q}'\mathcal{L}\mathcal{Q}'-z)^{-1}\mathcal{P}_2, \tag{31a}$$

where $\mathcal{P}$ projects on the space spanned by $\rho_{\vec{k}_1}\rho_{\vec{k}_2}$. Evaluation of the right-hand side of Eq. (31a) requires knowledge of the normalization functions

$$N_{\vec{k}_1\vec{k}_2,\vec{p}_1\vec{p}_2}=(\rho_{\vec{k}_1}\rho_{\vec{k}_2}|\rho_{\vec{p}_1}\rho_{\vec{p}_2}) \tag{31b}$$

and of the propagators

$$\psi_{\vec{k}_1\vec{k}_2,\vec{p}_1\vec{p}_2}(z)=(\rho_{\vec{k}_1}\rho_{k_2}|(\mathcal{Q}'\mathcal{L}\mathcal{Q}'-z)^{-1}|\rho_{\vec{p}_1}\rho_{p_2}). \tag{31c}$$

Since we are not interested in such fine-structure effects of ψ which might be due to roton-roton resonance scattering we approximate the two-mode propagation by the independent propagation of two single modes, i.e.,

$$\langle(e^{i\mathcal{Q}'\mathcal{L}\mathcal{Q}'t}\rho_{\vec{k}_1}\rho_{\vec{k}_2})^*\rho_{\vec{p}_1}\rho_{\vec{p}_2}\rangle \simeq\langle\rho_{\vec{k}_1}(t)^*\rho_{\vec{p}_1}\rangle\langle\rho_{\vec{k}_2}(t)^*\rho_{\vec{p}_2}\rangle+(\vec{p}_1-\vec{p}_2). \tag{31d}$$

A similar factorization is carried out for the reversed time order occurring in the definition of the scalar product. With Eqs. (5a) and (5b) one then finds for the approximation

$$\psi''_{\vec{k}_1\vec{k}_2,\vec{p}_1\vec{p}_2}(\omega)\simeq(\delta_{\vec{k}_1\vec{p}_1}\delta_{\vec{k}_2\vec{p}_2}+\vec{p}_1-\vec{p}_2)\psi''(k_1k_2\omega), \tag{32a}$$

where

$$\omega\psi''(k_1k_2\omega)=\frac{1}{\pi}\int d\omega_1\frac{1}{\pi}\int d\omega_2\,\pi\delta(\omega-\omega_1-\omega_2) \times\{[1+n(\omega_1)][1+n(\omega_2)]-n(\omega_1)n(\omega_2)\} \times\chi''(k_1\omega_1)\chi''(k_2\omega_2). \tag{32b}$$

Hence the two-mode propagator (31c) has been reduced approximately to a convolution of single-density correlation functions. The static response function (31b) is given in terms of ψ''[see Eqs. (7b) and (4a)]

$$N_{\vec{k}_1\vec{k}_2,\vec{p}_1\vec{p}_2}\simeq(\delta_{\vec{k}_1\vec{p}_1}\delta_{\vec{k}_2\vec{p}_2}+\vec{p}_1-\vec{p}_2)N(k_1k_2), \tag{32c}$$

where

$$N(k_1k_2)=\frac{1}{\pi}\int d\omega\,\psi''(k_1k_2\omega). \tag{32d}$$

As final result one arrives at the following approximation for expression (31a)

$$(\mathcal{Q}'\mathcal{L}\mathcal{Q}'-z)^{-1}\simeq\frac{1}{2}\sum_{\vec{k}_1\vec{k}_2}|\rho_{\vec{k}_1}\rho_{\vec{k}_2})\,N(k_1k_2)^{-1}\psi(k_1k_2z) \times N(k_1k_2)^{-1}(\rho_{\vec{k}_1}\rho_{\vec{k}_2}|. \tag{33}$$

B. Two-mode decay vertex

The determination of M according to Eqs. (23) and (33) requires the evaluation of the vertex

$$V(\vec{q}\,\vec{k}_1\vec{k}_2)=(\tau(\vec{q})|\rho_{\vec{k}_1}\rho_{\vec{k}_2})/N(k_1k_2). \tag{34a}$$

Momentum conservation yields zero unless $\vec{q}=\vec{k}_1+\vec{k}_2$. The first contribution to the numerator due to Eq. (23) is easy to calculate with Eqs. (11)

and (12)

$$(\mathfrak{L}^2\rho_{\vec{q}}|\rho_{\vec{k}_1}\rho_{\vec{k}_2}) = -\langle[q_\alpha j_\alpha(\vec{q})^*, \rho_{\vec{k}_1}\rho_{\vec{k}_2}]\rangle$$
$$= \delta_{\vec{q}_1,\vec{k}_1+\vec{k}_2}(1/m)[\vec{q}\vec{k}_1 s(k_2) + \vec{q}\vec{k}_2 s(k_1)]. \quad (34b)$$

The second contribution to the numerator is given by the static correlation $(\rho_{\vec{q}}|\rho_{\vec{k}_1}\rho_{\vec{k}_2})$. It is the change of the two-particle correlation $\langle\rho_{\vec{k}_1}\rho_{\vec{k}_2}\rangle$ due to an external zero-frequency field varying with wave number $\vec{q}$. According to Sec. IIA one can write

$$(\rho_{\vec{q}}|\rho_{\vec{k}_1}\rho_{\vec{k}_2}) = -\frac{1}{\pi}\int d\omega\langle\langle\rho^*_{\vec{q}};\ \rho_{\vec{k}_1}\rho_{\vec{k}_2}\rangle\rangle''_\omega\omega^{-1}. \quad (34c)$$

The quantities $N(k_1k_2)$ and $(\rho_{\vec{q}}|\rho_{\vec{k}_1}\rho_{\vec{k}_2})$ entering the vertex are only certain frequency averages and therefore the lowest approximation for the underlying susceptibilities can be considered as reasonable. To calculate the normalization function $N(k_1k_2)$ we substitute the Bijl-Feynman approximation (30) into Eqs. (32d) and (32b) to get at zero temperature

$$N(k_1k_2) \simeq 2s(k_1)s(k_2)[\epsilon_0(k_1)+\epsilon_0(k_2)]^{-1}. \quad (35)$$

Further, we replace $\Omega_0(q)$ in Eq. (23) by its zeroth approximation (1b) $\epsilon_0(q)$. To evaluate the three density correlation function (34c) we assume $\langle\langle\rho^*_{\vec{q}};\ \rho_{\vec{k}_1}\rho_{\vec{k}_2}\rangle\rangle''_\omega$ to have resonances at $\epsilon_0(q)$ and $\epsilon_0(k_1)+\epsilon_0(k_2)$. Hence one approximates

$$\langle\langle\rho^*_{\vec{q}};\ \rho_{\vec{k}_1}\rho_{\vec{k}_2}\rangle\rangle''_\omega \simeq \pi A\delta(\omega-\epsilon_0(q)) + \pi B\delta(\omega-\epsilon_0(k_1)-\epsilon_0(k_2)) - (\omega\to-\omega). \quad (36)$$

Here we have used $\langle\langle\rho^*_{\vec{q}};\ \rho_{\vec{k}_1}\rho_{\vec{k}_2}\rangle\rangle''_\omega$ to be odd in ω since $\rho(\vec{r})$ is Hermitian and invariant under time reversal. The coefficients A and B are determined by sum rules. For instance

$$(\mathfrak{L}^2\rho_{\vec{q}}|\rho_{\vec{k}_1}\rho_{\vec{k}_2}) = 2A\epsilon_0(q) + 2B[\epsilon_0(k_1)+\epsilon_0(k_2)]. \quad (37a)$$

The left-hand side of this relation is given by Eq. (34b). Furthermore, the fluctuation-dissipation theorem (5b) yields for zero temperature

$$\langle\rho^*_{\vec{q}}\rho_{\vec{k}_1}\rho_{\vec{k}_2}\rangle = A + B. \quad (37b)$$

The three-particle static correlation (34c) is then determined by

$$(\rho_{\vec{q}}|\rho_{\vec{k}_1}\rho_{\vec{k}_2}) = 2A/\epsilon_0(q) + 2B/[\epsilon_0(k_1)+\epsilon_0(k_2)]. \quad (37c)$$

Equations (37a)–(37c) express the three density correlation functions in terms of the equal time two particle and three-particle correlations.

For the vertex (34a) one then finds

$$V(\vec{q}_1\vec{k}_1\vec{k}_2) = \delta_{\vec{q},\vec{k}_1+\vec{k}_2}[\epsilon_0(q)+\epsilon_0(k_1)+\epsilon_0(k_2)]\left[\frac{\vec{q}\vec{k}_1 s(k_2)+\vec{q}\vec{k}_2 s(k_1)}{2ms(k_1)s(k_2)} - \epsilon_0(q)\frac{\langle\rho^*_{\vec{q}}\rho_{\vec{k}_1}\rho_{\vec{k}_2}\rangle}{s(k_1)s(k_2)}\right]. \quad (38)$$

To get the final formula for V some approximation for $\langle\rho^*_{\vec{q}}\rho_{\vec{k}_1}\rho_{\vec{k}_2}\rangle$ has to be made. The standard Kirkwood superposition approximation cannot be applied, since it yields a wrong long-wavelength behavior.[7] Jackson and Feenberg[10] have proposed the convolution approximation

$$\langle\rho^*_{\vec{p}}\rho_{\vec{k}_1}\rho_{\vec{k}_2}\rangle \simeq s(q)s(k_1)s(k_2), \quad (39)$$

which will be used in the following.

C. Self-consistency equations

The approximations specified above together with the formulas of Sec. II provide closed equations for the dynamical structure factor $S(q,\omega)$. At zero temperature one gets for Eq. (6)

$$S(q,\omega) = 2\chi''(q,\omega), \quad \omega > 0. \quad (40)$$

The susceptibility can be split into its single excitation part and a continuum contribution according to Eq. (27). The latter term follows for $\omega \neq \epsilon(q)$ from Eq. (21) to be

$$\chi''_c(q,\omega) = \frac{q^2}{m}\frac{\omega M''(q,\omega)}{[\omega^2-\Omega_0(q)^2+\omega M'(q,\omega)]^2+\omega^2M''(q,\omega)^2}. \quad (41)$$

It is determined by M'', M', and Ω_0. The single resonance parameters $\epsilon(q)$ and $Z(q)$ are given by $M'(q,\omega)$ and $\Omega_0(q)$ according to Eqs. (24) and (28). Since Eq. (29) provides a transcendental relation connecting $s(q)$ and $\Omega_0(q)$ everything has been reduced to $M(q,z)$ and $s(q)$. The real part $M'(q,\omega)$ of the polarization operator is determined by its imaginary part $M''(q,\omega)$ due to the causality relation (26). Finally, for the latter function in the preceding section the following formula has been derived:

$$M''(q,\omega) = \frac{m}{2q^2\omega}\sum_{\vec{p}}\frac{1}{\pi}\int d\epsilon\ \varphi(\vec{q},\vec{p})^2 \times\tfrac{1}{2}[\mathrm{sgn}(\epsilon)+\mathrm{sgn}(\omega-\epsilon)] \times\chi''(p,\epsilon)\chi''(|\vec{q}-\vec{p}|,\omega-\epsilon). \quad (42a)$$

According to Eq. (27) we split this expression into three contributions ($\omega > 0$):

$$M''(q,\omega) = M''_{1,1}(q,\omega) + M''_{1,c}(q,\omega) + M''_{c,c}(q,\omega), \quad (42b)$$

with the single-excitation–single-excitation term

$$M''_{1,1}(q,\omega)=\frac{m}{2q^2\omega}\sum_{\vec{p}}\varphi(\vec{q},\vec{p})^2\,Z(p)Z(|\vec{q}-\vec{p}|)\times\pi\delta(\omega-\epsilon(p)-\epsilon(|\vec{q}-\vec{p}|)),\tag{42c}$$

the single-excitation–continuum term

$$M''_{1,c}(q,\omega)=\frac{m}{2q^2\omega}\sum_{\vec{p}}\varphi(\vec{q},\vec{p})^2\times[Z(p)\chi''_c(|\vec{q}-\vec{p}|,\omega-\epsilon(p))+\vec{p}\to\vec{q}-\vec{p}],\tag{42d}$$

and the continuum-continuum term

$$M''_{c,c}(q,\omega)=\frac{m}{2q^2\omega}\sum_{p}\int_0^\omega d\epsilon\,\varphi(\vec{q},\vec{p})^2\times\chi''_c(p,\epsilon)\chi''_c(|\vec{q}-\vec{p}|,\omega-\epsilon).\tag{42e}$$

The vertex is expressed in terms of $s(q)$[see Eqs. (38), (39), and (1b)]

$$\varphi(\vec{q},\vec{p})=\frac{q^2}{2m}[\epsilon_0(q)+\epsilon_0(p)+\epsilon_0(|\vec{q}-\vec{p}|)]\times\left[\frac{\vec{q}\vec{p}}{q^2s(p)}+\frac{\vec{q}(\vec{q}-\vec{p})}{q^2s(|\vec{q}-\vec{p}|)}-1\right].\tag{43}$$

The static structure factor $s(q)$ we take from x-ray scattering experiments.[25] Since there are good first-principles calculations for $s(q)$[26] this procedure does not ruin our claim to present a microscopic theory. Equations (42d)–(42e) express M'' in terms of χ'' and so the system is closed.

The contents of the preceding set of Eqs. (41) to (43) is obvious. According to Eq. (21) density fluctuations feel a self-consistent static restoring force corresponding to the frequency $\Omega_0(q)$ and a coupling to the reservoir of the other modes in the system. The influence of the reservoir is described by the polarization operator $M(q,z)$ representing the correlations of the random force $\tau(\vec{q})$. The transfer of energy from the coherent motion to the incoherent one is approximated here by the decay of single modes into pairs according to Eq. (42a). The pair modes are real excitations of the system and have to be determined consistently with the excitations expressed by the poles of $\chi(q,z)$. The preceding self-consistency equations are similar in spirit to the ones suggested by Jackson[11] but a detailed comparison does not seem possible because of different mathematical frames.

IV. SOLUTION OF THE SELF-CONSISTENCY EQUATIONS

A. Iteration scheme

The Bijl-Feynman approximation $M_0(q,z)=0$ for the correlation function will be used as starting point of an iteration procedure for the self-consistency equations. However, a straightforward iteration is not successful as demonstrated in Appendix A. To avoid a mathematical instability of the iteration procedure it is necessary to switch on the decay vertex gradually. The instability and the modified iteration are discussed more explicitly in Appendix B analyzing a simplified mathematical model. So the following iteration scheme is set up. The nth approximation of the kernel M and static susceptibility determines the correlation function according to Eqs. (27), (28a), and (41),

$$\chi''_n(q\omega)/\pi s(q)=f_n(q)\delta(\omega-\epsilon_n(q))+\chi''_{cn}(q,\omega)/\pi s(q),\tag{44a}$$

where for $\omega\neq\epsilon_n(q)$

$$\frac{\chi''_{cn}(q\omega)}{\pi s(q)}=\frac{2\omega\epsilon_0(q)}{\pi}\frac{M''_n(q,\omega)}{[\omega^2-\Omega_{0n}(q)^2+\omega M'_n(q\omega)]^2+\omega^2M''_n(q,\omega)^2}.\tag{44b}$$

The nth approximation for the single excitation resonance follows from Eq. (24)

$$\Omega^2_{0n}(q)/\epsilon_n(q)-\epsilon_n(q)=M'_n(q,\epsilon_n(q)).\tag{44c}$$

The solution of the self-consistency equations of Sec. III C automatically obeys the two sum rules (14) and (15). Instead of fixing f_n according to Eq. (28b) one can use sum rules also. We found it most convenient to determine $f_n(q)$ with Eq. (29):

$$f_n(q)=1-\int_0^\infty d\omega\frac{\chi''_{cn}(q,\omega)}{\pi s(q)}.\tag{44d}$$

Then Eqs. (44b) and (44c) fix f_n,ϵ_n in terms of Ω_{0n}, i.e., $\chi''_n(q,\omega)$ is a given function of $\Omega_{0,n}$. To determine $\Omega_{0,n}$ one can use the f sum rule

$$\epsilon_0(q)=\epsilon_n(q)f_n(q)+\int_0^\infty d\omega\frac{\omega\chi''_{c,n}(q,\omega)}{\pi s(q)}.\tag{44e}$$

This transcendental equation can be solved graphically. With equal reason one can use sum rule (14) to fix $\Omega_{0,n}(q)$

$$\frac{\epsilon_0(q)}{\Omega_{0n}(q)^2}=\frac{f_n(q)}{\epsilon_n(q)}+\int_0^\infty d\omega\frac{\omega^{-1}\chi''_{c,n}(q,\omega)}{\pi s(q)}.\tag{44f}$$

We calculated $\Omega_{0,n}$ in such a way that the sum of numerical errors in solving Eqs. (44e) and (44f) was minimal. Having thus fixed $\chi''_n(q,\omega)$ one gets the $(n+1)$st approximation for the kernel from Eqs. (42a)–(42c)

$$M''_{n+1}(q,\omega)=\frac{m}{2q^2\omega}\sum_{\vec{p}}\frac{1}{\pi}\int_0^\omega d\epsilon\,\varphi_{n+1}(\vec{q},\vec{p})^2\chi''_n(p,\epsilon)\chi''_n\times(|\vec{q}-\vec{p}|,\omega-\epsilon).\tag{44g}$$

Here

$$\varphi_{n+1}(\vec{q},\vec{p})^2=\lambda_{n+1}\varphi(\vec{q},\vec{p})^2 \tag{44h}$$

is the vertex (43) switched on with the factor λ_n.

Eight iterations have been carried out. We have chosen $\lambda_1=\frac{2}{6},\lambda_2=\frac{3}{6},\lambda_4=\frac{4}{6},\lambda_5=\frac{5}{6}$, and $\lambda_n=1$ for $n\geq 6$. In Figs. 1(a) and 1(b) the results for ϵ_n and f_n are represented. The curves for the iteration 6, 7, and 8 demonstrate, that indeed a solution of the nonlinear equations of Sec. III has been found consistent within about 4%. With similar accuracy the three sum rules (14), (15), and (29) are fulfilled. No particular significance should be attributed to the iteration result for $n=1,\ldots,6$ but we find it satisfactory to show explicitly in Fig. 1 how the final result develops gradually starting with the simple Bijl-Feyman formulas $\epsilon_0(q)=q^2/2ms(q)$ and $f_0(q)=1$. The convergence is shown more clearly in Fig. 1(c) where for some representative values of q the iteration results are plotted in the $\epsilon-f$ plane. There we have also shown the result for the straightforward iteration with $\lambda_1=\lambda_2=1$.

B. Technical details

A computer has to be used in order to carry out the various integrals entering the iteration scheme of Eq. (44). The time necessary to evaluate $M'(q,\omega)$ as Hilbert transform (26) and the sum-rule contributions [44(d)–44(f)] is negligible compared to the time necessary to determine the convolutions in Eq. (44g). These convolutions have been carried out for 16–20 q values and 150–200 ω values for each iteration. The $M''_{1,c}(q,\omega)$ contribution (42d) and the $M''_{c,c}(q,\omega)$ term (42e) have been evaluated with a Gaussian integration procedure and linear interpolation of the integrand. The $M''_{c,c}(q,\omega)$ contribution turned out to be so small that it was sufficient to include it for the last iteration step only.

The most interesting contribution to $M''(q,\omega)$ is the decay part into two single excitations which, according to Eqs. (42c) and (43) reads

$$M''_{1,1}(q,\omega)=\frac{1}{\omega}\int_0^\infty dp\int_{|q-p|}^{q+p}dk\,C_q(p,k)\times\delta(\omega-\epsilon(p)-\epsilon(k)). \tag{45}$$

Here the sum in Eq. (42c) has been converted into an integral according to

$$\sum_{\vec{p}}\cdots=\frac{1}{(2\pi)^2 n}\int_0^\infty dp\int_{|q-p|}^{q+p}dk\frac{kp}{q}\cdots$$

with $n=0.0218$ Å^{-3} denoting the helium particle density. The coupling function is given by Eq. (43)

$$C_q(p,k)=[\epsilon_0(q)+\epsilon_0(k)+\epsilon_0(p)]^2\times[(q^2+p^2-k^2)s(k)+(q^2+k^2-p^2)s(p)-2q^2s(k)s(p)]^2f(p)f(k)kp/[128\pi q^3 s(p)s(k)mn]. \tag{46}$$

The integral in Eq. (45) is calculated with a modification of the Gilat and Raubenheimer technique.[27] One introduces a square grid (p_i,k_j) for the integration area with axis parallel to the integration boundaries $k=q+p$ and $k=|q-p|$ with a mesh area $\delta^2=(0.05\ \text{Å}^{-1})^2$:

$$\int_0^\infty dp\int_{|q-p|}^{q+p}dk\,C_q(p,k)\delta(\omega-E(p,k))=\sum_{ij}I_{ij}(\omega), \tag{47a}$$

$$I_{ij}(\omega)=\int_0^1 du\int_0^1 dv\,C_{ij}(u,v)\delta(\omega-E_{ij}(u,v)). \tag{47b}$$

Here (u,v) denote the integration variables for the area (i,j), $C_{ij}(u,v)$ abbreviates the corresponding coupling function, $E_{ij}(u,v)=\epsilon(k)+\epsilon(p)$ is the frequency sum for momenta in the area (i,j). The integral over v can be carried out explicitly

$$\int dv\,C_{ij}(u,v)\delta(\omega-E_{ij}(u,v))=C_{ij}(u,v^0(u,\omega))\left|\frac{\partial E_{ij}(u,v^0(u,\omega))}{\partial v}\right|^{-1} \tag{47c}$$

if the zero v^0 of the equation $\omega=E_{ij}(u,v^0)$ can be found elementarily. For this end we have used the bilinear interpolation formula $[E_{ij}=E(p_i,k_j)]$:

$$E_{ij}(u,v)\approx E_{ij}(1-u)(1-v)+E_{i,j+1}(1-u)v\times E_{i+1,j}u(1-v)+E_{i+1,j+1}uv. \tag{47d}$$

For the integration over u restricted by the requirements $0\leq u\leq 1$ and $0\leq v^0(u,\omega)\leq 1$ we approximated the smooth function $C_{ij}(u,v^0)$ on the right-hand side of Eq. (47c) by its value in the middle of the integration interval; the remaining u integral was carried out elementarily. The frequency steps have been chosed as 1 deg.

An IBM 360/91 machine has been used. For one iteration step, 3 min of calculation time was necessary: 1 min for the $M''_{1,1}$ contribution and 2 min for the $M''_{1,c}$ term. For the last iteration step the accuracy has been improved (frequencies in steps of 0.25 deg) with a corresponding increase of computer time used.

V. DISCUSSION

A. Elementary excitations

In Fig. 2 the result for $\epsilon(q)$ is plotted in comparison with experiment[21] and earlier theo-

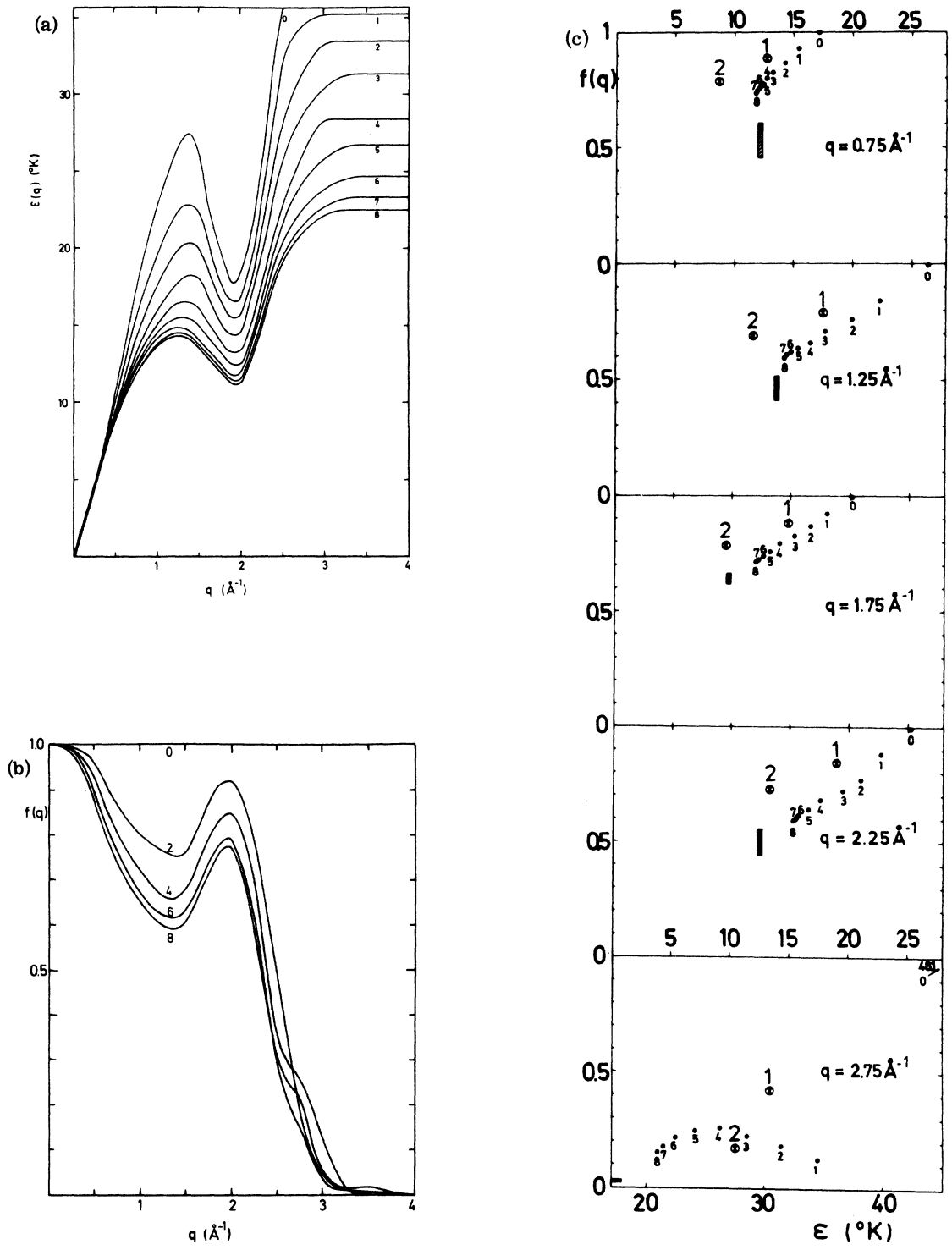

FIG. 1. (a) Excitation spectra $\epsilon_n(q)$ for the iteration steps $n=0, 1, \ldots, 8$. (b) Strength factors $f_n(q)$ for the iteration steps $n=0, 2, \ldots, 8$. (c) Iteration results $\epsilon_n - f_n$ for various q values. The crosses ⊗ mark the results for the straight forward iteration with $\lambda_1=\lambda_2=1$. Shaded area is the experimental result (Ref. 21).

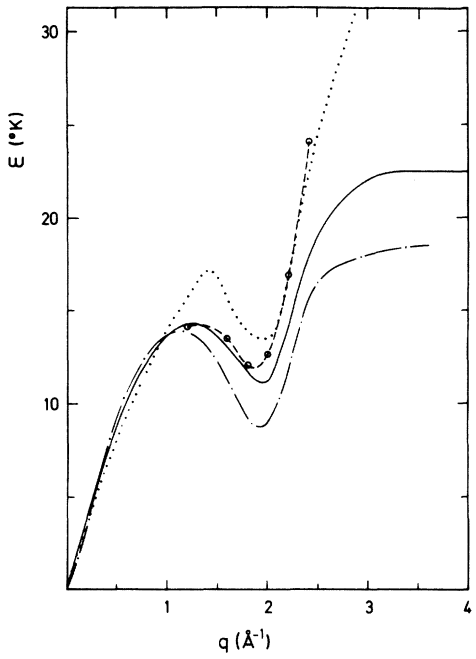

FIG. 2. Excitation spectrum $\epsilon(q)$ (solid line) compared with the experimental result of Cowley and Woods (Ref. 21) (dashed-dotted curve). The dashed line is the Feynman-Cohen result (Ref. 7); the dotted line is the Jackson-Feenberg curve (Refs. 10, 11, and 28).

ries.[7,11,28] For wave numbers between 0 and 2 Å^{-1} only a slight improvement has been achieved by the present work. The roton energy is $\Delta \simeq 11$ °K in comparison with 11.9 °K of Feynman and Cohen's calculation. It is about 20% above the experimental value. While the earlier work has an error increasing rapidly with q larger then 2 Å^{-1}, the present result shows the Pitaevskij bending in qualitative agreement with experiment. The relative error of $\epsilon(q)$ does not increase with momentum. The spectrum terminates at about 4 Å^{-1}. The qualitative features of $\epsilon(q)$ have been understood before.[7,8]

The directly measurable single excitation intensity $Z(q)$ is shown in Fig. 3(a). In Fig. 3(b) the result for the strength factor $f(q)$ is plotted. The main contribution to $M''(q,\omega)$ due to $M''_{1,1}(q,\omega)$ starts to be appreciable at the Pitaevskij singularity $\omega = 2\Delta$. There M' diverges logarithmically and $\partial M'/\partial\omega$ even stronger. The greater $\Omega_0(q) \simeq \epsilon_0(q)$ the closer $\epsilon(q)$ comes to 2Δ and the stronger will be the renormalization of $f(q)$. This explains why $f(q = 1$ Å$^{-1})$ is smaller than $f(q = 2$ Å$^{-1})$ and also why $f(q)$ drops rapidly towards zero for q exceeding 2 Å^{-1}. So the characteristic oscillation of the experimental $f(q)$ is explained qualitatively by the

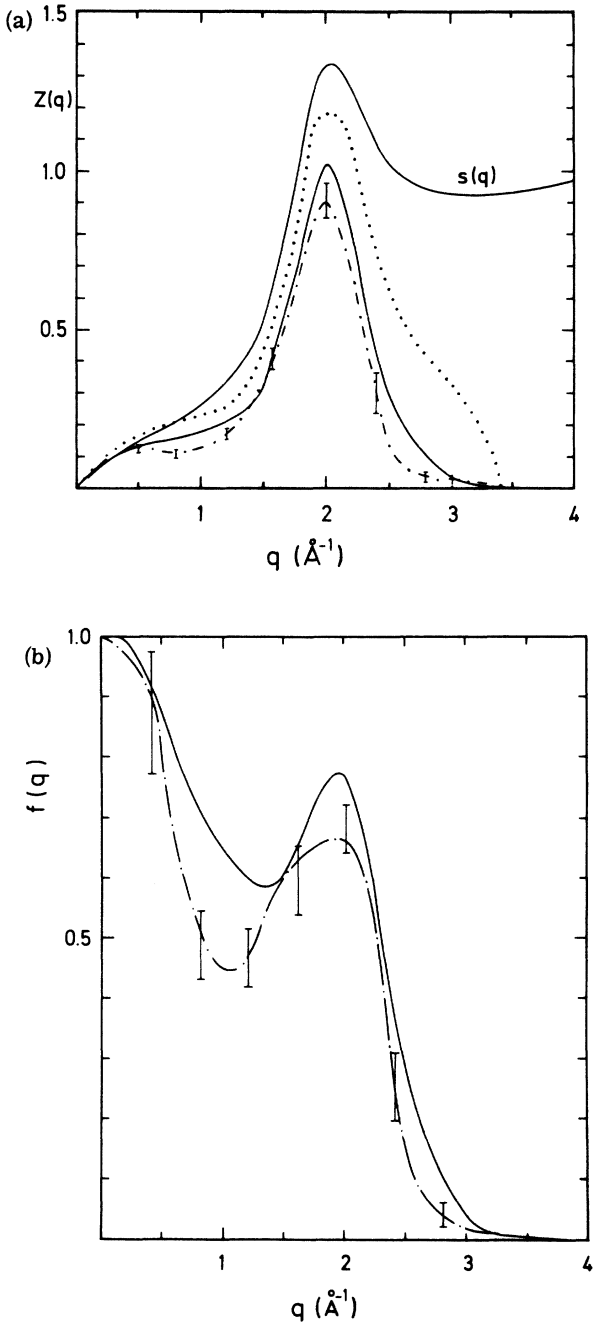

FIG. 3. (a) Single excitation strength $Z(q) = f(q)s(q)$ (solid curve) compared with experiment (Ref. 21) (dashed dotted). The dotted curve is the Jackson result (Ref. 11). The structure factor $Z_0(q) = s(q)$ used here is due to Achter and Meyer and Hallock (Ref. 25). (b) Strength factor $f(q)$ (full curve) compared with experiment (Ref. 21).

present theory. In comparison with experiment the errors of $f(q)$ are of the same order as those for $\epsilon(q)$.

The static susceptibility $\chi_0(q)$ or equivalently the

corresponding frequency $\Omega_0(q)$ shown in Fig. 4 yields the inverse first frequency moment of the dynamical structure factor $S(q,\omega)$. Like $1-f(q)$ the frequency difference $\epsilon_0(q)-\Omega_0(q)$ gives some information about the continuous excitation spectrum $S_c(q,\omega)$.

Finally, let us stress one feature already obvious from Figs. 2–4. Expanding the vertex (43) for fixed p in the limit $\vec{q}\to 0$ one obtains $\varphi(\vec{q}\to 0,\vec{p}) = \bar{\varphi}(\vec{p})q^2$ and hence Eq. (42c) yields

$$M''(q,\omega) = O(q^2) \tag{48a}$$

for the 1-1 contribution. Equation (41) then leads to

$$\chi_c''(q,\omega) = (q^2/m\omega^3)M''(q,\omega), \quad q\to 0. \tag{48b}$$

Hence the $1,C$ and C,C terms do not change Eq. (48a). The result $\chi_c''(q,\omega) = O(q^4)$ is in agreement with the general reasoning of Miller *et al.*[13] The sum rules (14), (15), and (29) then yield

$$\epsilon_0(q) = \epsilon(q) = \Omega_0(q);\ f(q) = 1 \text{ for } q\to 0. \tag{48c}$$

There are no renormalization effects in the long-wavelength limit. Also one gets[4,13] $s(q) = aq$ with $a = 1/2mc$ and c denoting the sound velocity.

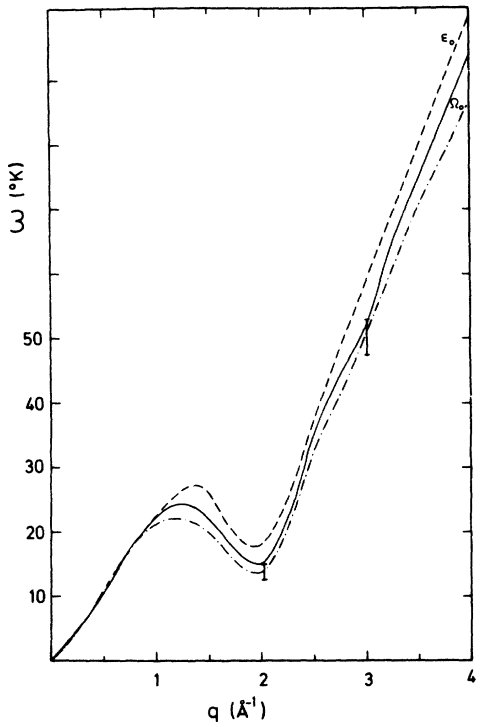

FIG. 4. Characteristic static frequency $\Omega_0(q)$ (solid curve) compared with the experimental results of Cowley and Woods (Ref. 21) (dashed-dotted line). The dashed curve is $\epsilon_0(q)$.

B. Pitaevskij singularities

In Fig. 5 the three contributions to $M''(q,\omega)$ according to Eqs. (42) are compared. For momenta q below 2.5 Å^{-1} the strength factors f entering Eq. (46) are rather big; therefore the $M''_{1,1}(q,\omega)$ term dominates and $M''_{c,c}(q,\omega)$ is very small. For larger momenta the continuum-continuum contribution becomes important. The convolution integrals for $M''_{1,c}(q,\omega)$ and $M''_{c,c}(q,\omega)$ yield rather smooth functions; the structure of $\chi_c''(q,\omega)$ is washed out.

The function $M''_{1,1}(q,\omega)$ exhibits a lot of structure

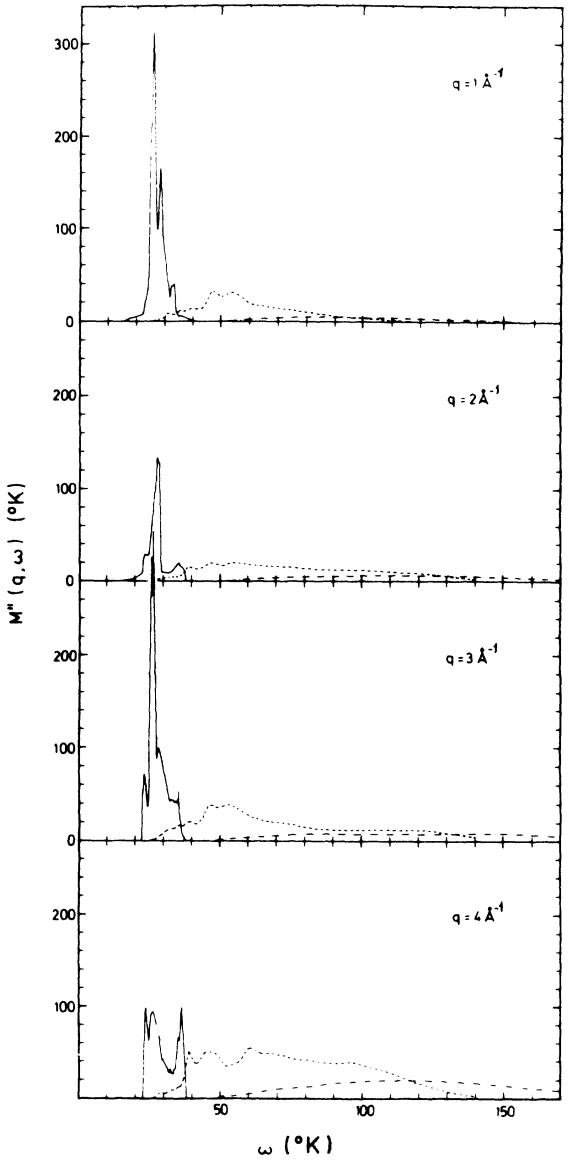

FIG. 5. Three contributions $M''_{1,1}(q,\omega)$ (solid curve), $M''_{1,c}(q,\omega)$ (dashed curve), and $M''_{c,c}(q,\omega)$ (dashed-dotted curve) to the imaginary part of the polarization operator.

due to opening and closing of scattering channels. The various singularities have been classified by Pitaevskij.[8]

Case a. The simplest singularities are due to the emission of soft phonons. They are given by the $p \to 0$, $k \to q$ contributions to the decay integral (45). For the near threshold asymptotic behavior one estimates

$$M_a''(q,\omega) \propto \int dp \int_{-p}^{p} dx p^2 \delta(\omega - \epsilon(q) - v(q)x - cp)$$

using the expansions $\epsilon(p) = cp$, $s(p) = cp$, $\epsilon(k) = \epsilon(q) + v(q)x$. A group velocity $v(q) = \partial\epsilon(q)/\partial q$ exceeding the sound velocity c causes $M_a''(q,\omega)$ to be nonzero for $\omega < \epsilon(q)$, i.e., elementary excitations would be damped by Čerenkov emission of sound. In agreement with experiment this situation does not occur for the spectrum calculated by the preceding theory and $q \geq 0.25$ Å^{-1}. Since $v(q) < c$ the type a singularity is situated on the resonance $\epsilon(q)$ and one finds

$$M_a''(q,\omega) = A(q)[\omega - \epsilon(q)]^3 \Theta(\omega - \epsilon(q)). \tag{49}$$

This small contribution can be seen for $q = 1$ or 2 Å^{-1} in Fig. 6(a). The anomaly in $M_a'(q,\omega)$ is a divergent third derivative which does not show up in Fig. 6(b).

Case b. Square-root branch points in $M(q,z)$ due to those thresholds with decay modes having equal or opposite group velocity, i.e., $k = q + p$ or $k = (q - p)$ and $v(k) = \pm v(p)$, are numerous and difficult to localize. Therefore we restrict ourselves to the simplest example: namely $k = p = \frac{1}{2}q$. Expanding around $\frac{1}{2}q$ one easily discusses the integral (45)

$$M_b''(q,\omega) \propto \int dp \int dk \delta(\omega - 2\epsilon(\tfrac{1}{2}q) - v(\tfrac{1}{2}q)(\delta p + \delta k) - \tfrac{1}{2}b(\tfrac{1}{2}q)(\delta p^2 + \delta k^2)).$$

Here $b(q) = \partial^2\epsilon(q)/\partial q^2$ is the curvature of the dispersion curve. There are four possibilities. First, $v(\frac{1}{2}q) > 0$ and $b(\frac{1}{2}q) < 0$ yields as singular part

$$M_{b1}''(q,\omega) = -B_1(q)[2\epsilon(\tfrac{1}{2}q) - \omega]^{1/2}\Theta(2\epsilon(\tfrac{1}{2}q) - \omega). \tag{50a}$$

Second, for $v(\frac{1}{2}q) < 0$ and $b(\frac{1}{2}q) < 0$ one finds

$$M_{b2}''(q,\omega) = B_2(q)[2\epsilon(\tfrac{1}{2}q) - \omega]^{1/2}\Theta(2\epsilon(\tfrac{1}{2}q) - \omega). \tag{50b}$$

Third, $v(\frac{1}{2}q) < 0$ and $b(\frac{1}{2}q) > 0$ yields

$$M_{b3}''(q,\omega) = -B_3(q)[\omega - 2\epsilon(\tfrac{1}{2}q)]^{1/2}\Theta(\omega - 2\epsilon(\tfrac{1}{2}q)). \tag{50c}$$

Finally, $v(\frac{1}{2}q) > 0$ and $b(\frac{1}{2}q) > 0$ leads to

$$M_{b4}''(q,\omega) = B_4(q)[\omega - 2\epsilon(\tfrac{1}{2}q)]^{1/2}\Theta(\omega - 2\epsilon(\tfrac{1}{2}q)). \tag{50d}$$

In all formulas the coefficients B are understood as positive. Some of the square roots are to be seen in Fig. 6; in particular $b4$ marks the lower bound of $M''(q,\omega) \neq 0$ for momenta around 4 Å^{-1}. The anomalies in $M'(q,\omega)$ in case b are symmetric square-root functions.

Case c. There is the analog of Van Hove singularities in the density of states function of two-dimensional systems whenever $E(p,k) = \epsilon(p) + \epsilon(k)$ in Eq. (45) exhibits a stationary point. This is the case if the group velocity of both decay states vanish. There are three possibilities. First, both decay excitations are rotons; $E(p,k)$ has a minimum 2Δ and Eq. (45) yields

$$M_{c1}''(q,\omega) = C_1(q)\Theta(\omega - 2\Delta). \tag{51a}$$

$C_1(q)$ is positive for $0 < q \leq 2k_0$; $k_0 \simeq 1.9$ Å^{-1} is the roton momentum. Figure 6(a) demonstrates, that $C_1(q)$ increases with q. The discontinuity is much more pronounced for q around 3 Å^{-1} than for q around 1 Å^{-1}. Second, both decay excitations can be maxons; $E(p,k)$ has a maximum $2\Delta' \simeq 29$ °K. One has

$$M_{c2}''(q,\omega) = C_2(q)\Theta(2\Delta' - \omega), \tag{51b}$$

with $C_2(q) > 0$ for $0 < q \leq 2k_0'$; $k_0' \simeq 1.25$ Å^{-1} is the maxon momentum; the discontinuities in the imaginary part imply symmetric logarithmic singularities in the real part $M'(q,\omega)$. In case $c1$ $M'(q,\omega)$ diverges towards plus infinity and in case $c2$ towards minus infinity. Third, one excitation can be a maxon and the other one a roton; $E(p,k)$ has a saddle point at $\Delta + \Delta'$. One finds a logarithmic singularity for the integral (45)

$$M_{c3}''(q,\omega) = C_3(q)\log|\omega - \Delta - \Delta'| \tag{51c}$$

and a corresponding discontinuity in the real part $M_{c3}'(q,\omega)$. $C_3(q)$ is positive for 0.6 Å$^{-1} \simeq k_0 - k_0' \leq q \leq k_0 + k_0' \simeq 3.1$ Å^{-1}.

The Pitaevskij classification is based on the tacit assumption that all functions entering the decay integral (45) depend analytically on the momenta. A nonanalyticity of $\epsilon(p)$ at p^*, for instance, would lead to further singularities of $M''(q,\omega)$. To make this point explicit let us assume $\epsilon(p)$ to be parabolic around k_0 but linear for $k_0 < p^* \leq p$. Then elementary discussion of Eq. (45) yields a singularity of the form

$$M_d''(q,\omega) = \{-D(q)[\omega - \epsilon(p^*)]^{1/2}\Theta(\omega - \epsilon(p^*)) + D'(q)[\omega - \epsilon(p^*)]\}. \tag{52}$$

This *case d* singularity (52) describes a hole on a smooth background. Further singularities of this case could be constructed for $p^* < k_0$ or choosing p^* near the maxon. The actual spectrum $\epsilon(p)$ shown in Fig. 2, indeed indicates a practical change

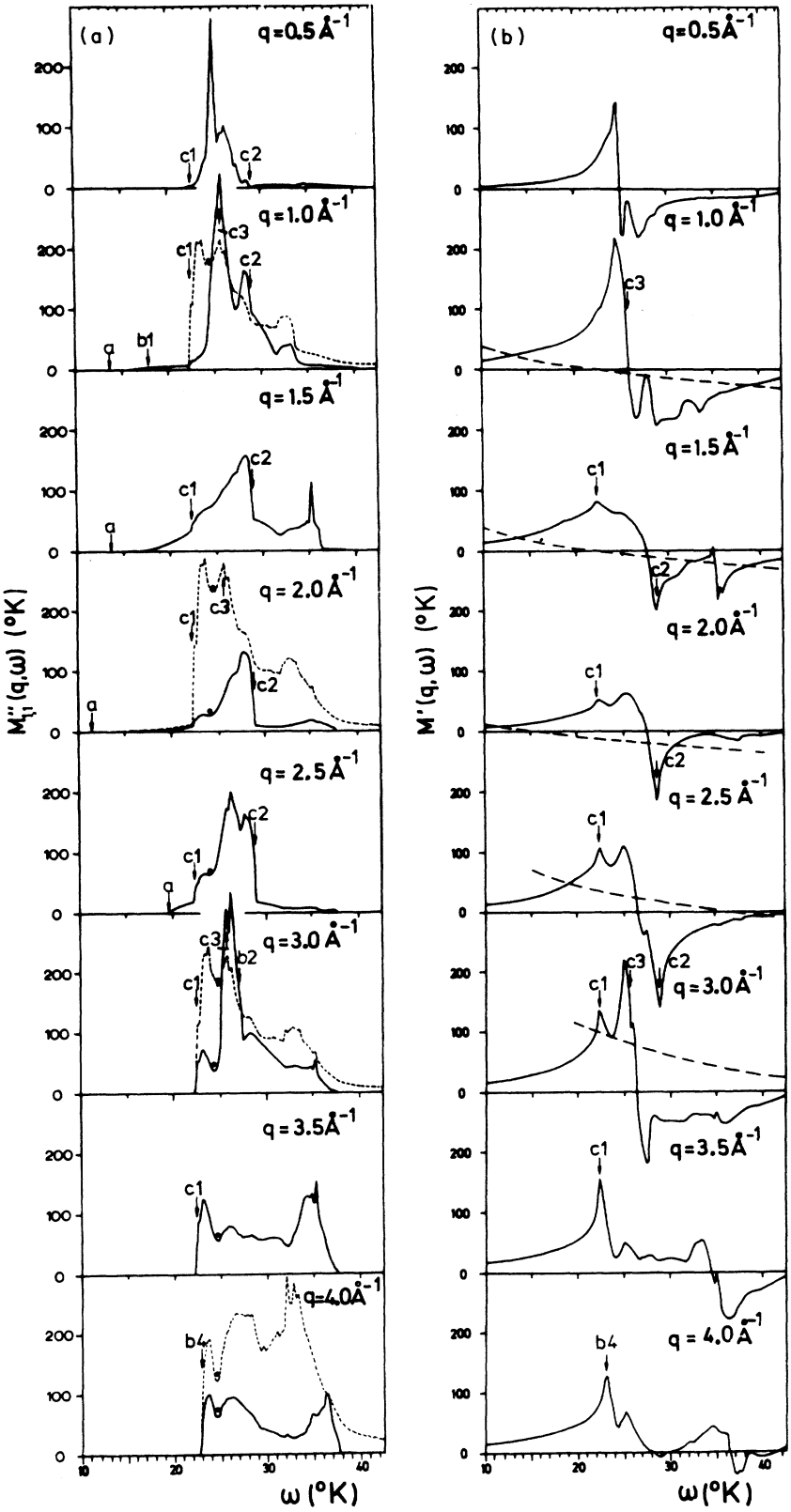

FIG. 6. (a) Single-excitation-single-excitation contribution to the imaginary part of the polarization operator $M''_{1,1}(q,\omega)$. Some Pitaevskij singularities are indicated by arrows. The dashed lines are the phase-space contributions only multiplied by 10^5 (for $q=1$ Å^{-1}), 10^6 (for $q=2$ Å^{-1}), 3×10^6 (for $q=3$ Å^{-1}), and 2×10^7 (for $q=4$ Å^{-1}), respectively. The ● mark the holes due to case d singularities. (b) Real part of the polarization operator $M'(q,\omega)$. Some Pitaevskij singularities are indicated by arrows. The dashed lines are the curves $\Omega_0(q)^2/\omega-\omega$.

from quadratic to linear behavior at $p^* \simeq 2.2$ Å^{-1}. The corresponding hole (52) is clearly visible in Fig. 6a for $q = 3.0, 3.5$ and 4.0 Å^{-1}. The case d singularity together with the $c1$ and $b4$ singularities thus are the explanation of the pronounced low-frequency peak of $M''_{1,1}(q,\omega)$ for momenta between 3.0 Å^{-1} and 4.5 Å^{-1}.

It should be stressed, that the momentum dependence of the decay vertex in Eq. (45) is very important. To elucidate this point the pure phase-space contribution to the decay integral (45) is shown by dashed curves in Fig. 6(a) for some momenta. These curves, obtained by putting $\varphi(\vec{q},\vec{p}) = 1$ in Eq. (42c), show the case c singularities clearly, while, e.g., for q between 1.5 Å^{-1} and 2.5 Å^{-1} $c3$ is not visible in the realistic calculation. While the phase-space contribution for $q = 4$ Å^{-1} is at least similar to the realistic function, it is quite different from $M''_{1,1}(q,\omega)$ for $q = 2$ Å^{-1}.

In discussing Pitaevskij singularities involving rotons it is also of importance to be aware of the variation of the strength factor $f(q)$. As explained in the preceding section and shown in Fig. 3(b), $f(q)$ drops rapidly for q increasing above 2 Å^{-1}. Practically there is a cut off for q around 2.7 Å^{-1}. So, after opening of the roton-roton scattering one expects a drop of $M''(q,\omega)$ due to the cut off mentioned. This explains for instance the decrease of $M''_{1,1}(q,\omega)$ for $q = 4$ Å^{-1} for frequencies between 25 and 30 °K.

C. Continuum $S_c(q,\omega)$

The shape of the continuum part of the dynamical structure factor $S_c(q,\omega)$ is a direct and elementary consequence of the properties of $\Omega_0(q)$ and $M''(q,\omega)$. The total percentage of neutrons creating multiple excitations is given by $1-f(q)$. The dominant resonances in $S_c(q,\omega)$ according to Eq. (41) are given by the zeros of the equation

$$\Omega_0(q)^2/\Omega(q) = M'(q,\Omega(q)). \tag{53a}$$

If it is allowed to approximate the functions in the preceding equations by the first Taylor coefficients one finds for the strength of the resonance similar to Eq. (28b)

$$F(q) = \frac{2\epsilon_0(q)/\Omega(q)}{1+\Omega_0^2(q)/\Omega^2(q) + \partial M'(q,\Omega(q))/\partial\omega} \tag{53b}$$

and the resonance half width is given by

$$\Gamma(q) = \tfrac{1}{2}F(q)[\Omega(q)/\epsilon_0(q)]M''(q,\Omega(q)). \tag{53c}$$

These formulas apply if the resonance can be approximated by a Lorentzian

$$\frac{\chi_c''(q,\omega)}{s(q)} \simeq \frac{\Gamma(q)}{[\omega-\Omega(q)]^2+\Gamma(q)^2}F(q). \tag{53d}$$

Although the preceding approximations are rather poor ones as demonstrated by Fig. 7 they help for a qualitative discussion. Only those solutions of Eq. (52a) with $\partial M'(q,\Omega(q))/\partial\omega > 0$ are important since otherwise the width $\Gamma(q)$ is too big.

Roughly $M''(q,\omega)$ is located between 2Δ and $2\Delta'$ and so $M'(q,\omega)$ is positive and increasing for $\omega < \Delta$ and negative and increasing for large ω. So one gets besides the elementary excitation resonance for low frequencies also a high-frequency solution of Eq. (53a). For large q this resonance is close to $\Omega_0(q) \simeq \epsilon_0(q)$ and the width is given by $\Gamma(q) \simeq M''(q,\epsilon_0(q))$. Decreasing q from 4 Å^{-1} to 2 Å^{-1} this resonance decreases and becomes sharper as shown in Fig. 8. For q decreasing below 2 Å^{-1} the resonance does not decrease because of a repulsion effect between the level $\Omega_0(q)$ and the double excitation states.

Function $M''(q,\omega)$ exhibits a resonance structure and this yields a further solution of Eq. (52a) as indicated in Fig. 6b. So we predict, at least for some momenta, a double peak structure of $\chi_c''(q,\omega)$. It should be worthwhile to check this consequence of the present theory by neutron scattering experiments. The many small bumps to be seen in Fig. 8 are due to the strong variation of $M''(q,\omega)$.

It should be remembered that the frequency steps underlying Figs. 6 and 7 are 0.25 °K. So one can not take serious anomalies on a frequency scale of 0.5 °K; such anomalies might be purely due to interpolation and rounding errors. For example, the case a singularity (49) implies an increase of $S_c(q,\omega)$ proportional to $[\omega-\epsilon(q)]\Theta(\omega-\epsilon(q))$. It can be seen quite nicely in Fig. 7 for $q = 1.5$ Å^{-1}. For $q = 2.25$ Å^{-1} or $q = 2.75$ Å^{-1}, however, the continuum yields an erroneous high-frequency tail of the elementary excitation peak. We have not eliminated this artifact, since in experiment due to finite resolutions and nonzero temperature, such tails will be observed anyway.

D. Bending phenomenon

Let us consider once more the frequency range close to 2Δ. The logarithmic singularity of $M'(q,\omega)$ due to the discontinuity (51a) prevents the spectrum $\epsilon(q)$ to cross 2Δ.[8] As soon as $\Omega_0(q) \simeq \epsilon_0(q)$ approaches 2Δ for $q > 2.3$ Å^{-1} $\epsilon(q)$ bends. In the present theory, neglecting vertex corrections, $\epsilon(q)$ has a case b endpoint[8] slightly above $2k_0 \simeq 3.8$ Å^{-1}. Since $\epsilon_0(q)$ increases so quickly, however, the strength $f(q)$, according to Eq. (28b) drops sharply. So the inelastic neutron cross section for the emission of a single excitation of liquid helium, being proportional to

$$S_1(q,\omega)/s(q) = \pi f(q)\delta(\omega-\epsilon(q)) \tag{54a}$$

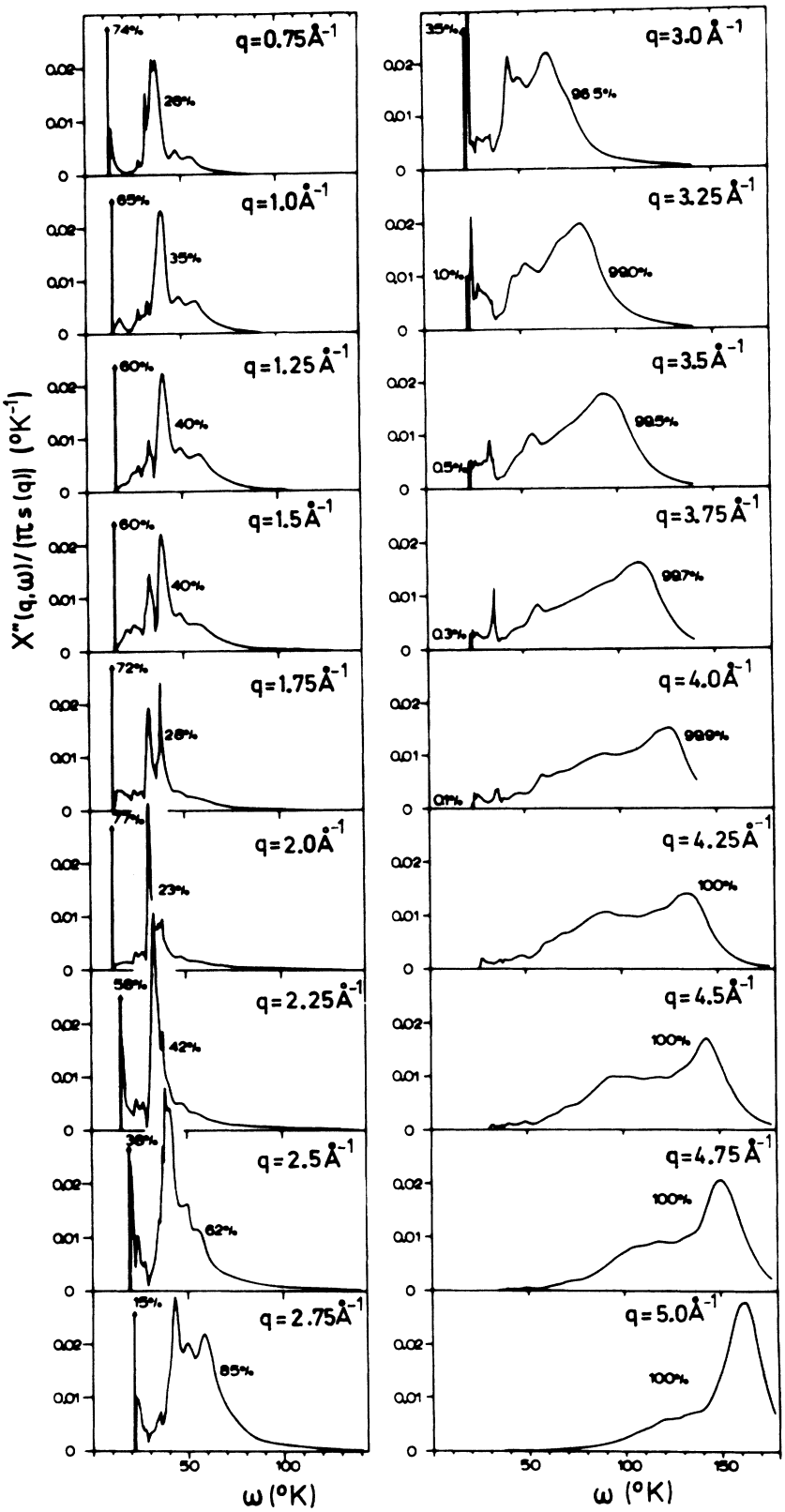

FIG. 7. Normalized dynamical structure factor $S(q,\omega)/2\pi s(q) = \chi''(q,\omega)/\pi s(q)$.

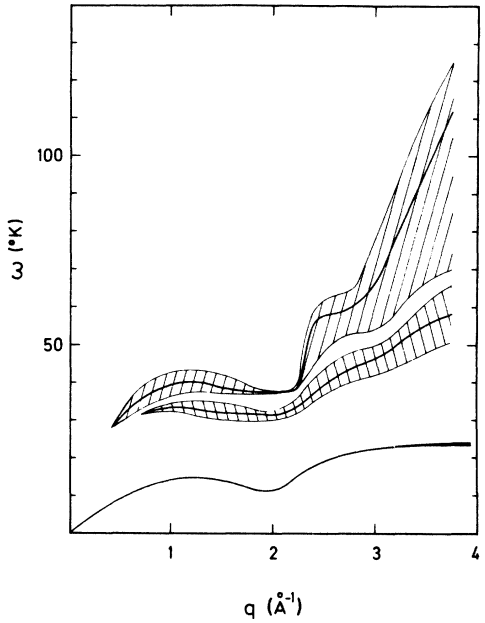

FIG. 8. Resonances of the dynamical structure factor $S(q,\omega)$. The low curve is the elementary excitation spectrum. The two upper curves are the dominant resonances of $S_c(q,\omega)$ with indicated half-width.

is very small for $q \simeq 3.5$ Å^{-1}.

The solution of Eq. (53a) slightly above 2Δ, which is due to the branch of the symmetric logarithm for $\omega > 2\Delta$, does not yield a resonance because $\partial M'/\partial\omega$ is negative there.

Approximately, one can write the continuum part of the structure factor according to Eq. (41)

$$\frac{S_3(q,\omega)}{s(q)} \simeq 2\omega\epsilon_0(q)\frac{1}{[\omega^2-\Omega_0^2(q)]^2}M''(q,\omega). \qquad (54b)$$

Remembering Eq. (42a) as the relevant contribution, one can interpret Eq. (54b) as follows. The neutron is scattered by a virtual excitation. The prefactor of $M''(q,\omega)$ in Eq. (54) is the square of the off-shell propagator of this intermediate boson. The intermediate boson then decays with a vertex proportional to $\varphi(\vec{q},\vec{p})$ into two real liquid-helium excitations with momenta $\vec{p}$ and $\vec{q}-\vec{p}$.

In Sec. IV B it has been shown that for q between 3.0 and 4.5 Å^{-1} the cross section (54b) exhibits a resonance above 2Δ and $2\epsilon(q,2)$, respectively. This resonance is visible on Fig. 7. It is also evident from the figure, that the resonance strength in the bending region is comparable with the strength $f(q)$ of the single excitation peak.

In the experiment a convolution of the sum of the cross sections $S_1(q,\omega)$ and $S_2(q,\omega)$ with the resolution curve is observed. Assuming a Gaussian resolution of half-height half-width of 1 °K the resulting cross section is shown in Fig. 9(a). For

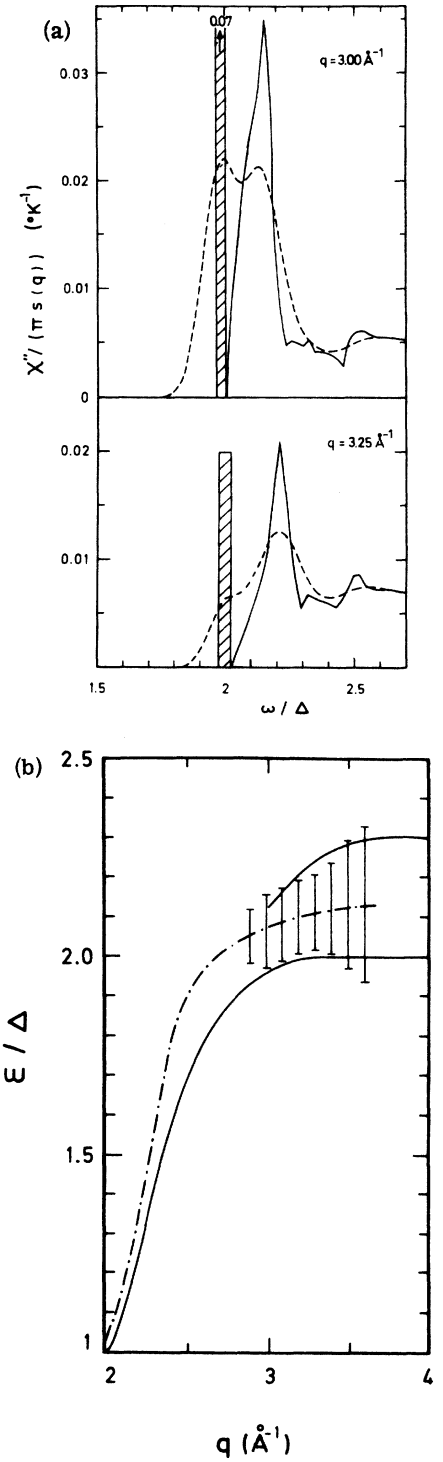

FIG. 9. (a) Solid curves are the normalized dynamical structure factor for $q = 3.0$ and 3.25 Å^{-1}. The dashed curves are the convolutions with a resolution function of half-width 2 °K. (b) Dashed-dotted curve is the experimentally observed (Ref. 21) dominant resonance. The solid curves are the theoretical elementary excitation spectrum and the two-excitation resonance, respectively.

$q = 3.0$ Å^{-1} the smeared out single-excitation resonance can just be seen as separated from the smeared out two-excitation resonance. Already for $q = 3.25$ Å^{-1} the elementary excitation is no longer detectable but the two excitation resonances (54b) above 2Δ dominates the curve. So the present theory explains why the effective resonance observed by Cowley and Woods[21] exceeds 2Δ for momenta exceeding about 3 Å^{-1}.

ACKNOWLEDGMENTS

Stimulating conversations with Professor P. C. Hohenberg are acknowledged. We also thank Professor P. Wölfle very much for many discussions and helpful suggestions.

APPENDIX A: FIRST APPROXIMATION

Considering the Bijl-Feynman variational solution $M(q,z) = 0$ as zeroth approximation one would get a first approximation by substituting

$$\chi_0''(q,\omega) = s(q)\pi\delta(\omega - \epsilon_0(q)) \tag{A1}$$

into Eq. (42) for $M''(q,\omega)$:

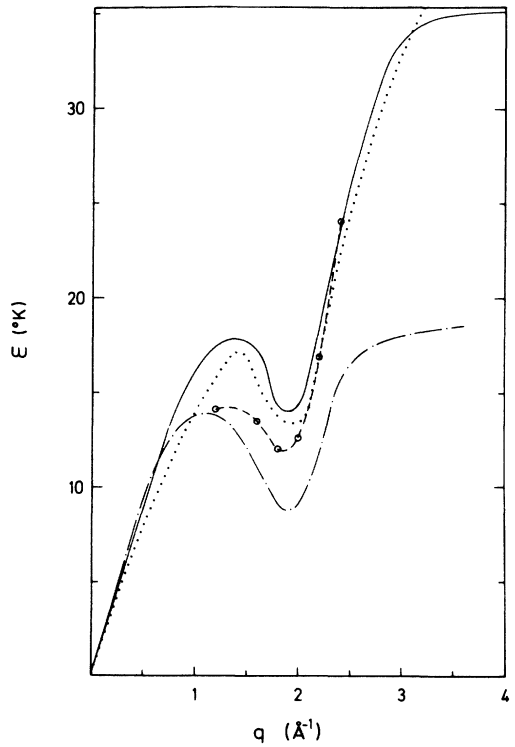

FIG. 10. First approximation $\epsilon_1(q)$ for the excitation spectrum. Dotted curve is the result of Jackson (Ref. 11); dashed curve is the Feynman-Cohen spectrum (Ref. 7). Dashed-dotted line is the experimental result (Ref. 21).

$$M_1''(q,\omega) = \left(\frac{m}{2\omega}\right)\sum_{\vec{p}} \varphi(\vec{q},\vec{p})^2\, \pi s(p) s(|\vec{q}-\vec{p}|) \times \delta(\omega - \epsilon_0(p) - \epsilon_0(|\vec{q}-\vec{p}|)). \tag{A2}$$

The real part of the polarization operator is obtained readily from Eq. (26)

$$M_1'(q,\omega) = (m\omega)\sum_{\vec{p}} \varphi(\vec{q},\vec{p})^2 s(p) s(|\vec{q}-\vec{p}|) \times [\epsilon_0(p) + \epsilon_0(|\vec{q}-\vec{p}|)]^{-1} \times [\epsilon^0(p) + \epsilon^0(|\vec{q}-\vec{p}|)^2 - \omega^2]^{-1}. \tag{A3}$$

Then the formula (24) for the first approximation of the excitation spectrum $\epsilon_1(q)$ has the typical form of a second-order Born approximation expression. The first approximation $Z_1(q)$ follows from (28). $\epsilon_1(q)$, $Z_1(q)$ and $\chi_{c1}''(q,\omega)$ are given in terms of $\Omega_0(q)$ whose first approximation $\Omega_{01}(q)$ is obtained then by solving Eq. (29). The result for the excitation spectrum is represented as full curve in Fig. 10; it is practically identical with the result of Jackson and Feenberg, showing that there are no real contradictions between the present theory and the earlier approaches[10,11] for $q < 3$ Å^{-1}.

The result $\chi_1(q,z)$ is not a solution of the self-consistency equations of Sec. III C, of course. On the contrary, since there is a large difference between $\epsilon_0(q)$ and $\epsilon_1(q)$ one would expect the first approximation to be a rather crude one. A reasonable statement concerning the error can be made only by working out the next correction. This has been done with the result, that $\epsilon_2(q)$ differs considerably from $\epsilon_1(q)$. $\epsilon_3(q)$ differs considerably from $\epsilon_2(q)$ and is considerably below the experimental spectrum, etc. Indeed the straightforward iteration seems to be converge toward the collapse solution $\epsilon(q) \simeq 0$. Hence we conclude: either there is no reasonable solution for the self-consistency equations or there is one but it cannot be obtained by the straightforward iteration procedure discussed. In any case, there is no justification to attribute a physical meaning to the first approximation.

APPENDIX B: SIMPLIFIED MODEL

To understand the origin of the iteration collapse and to get an idea how to solve the self-consistency equations let us consider a simplified mathematical model. Let us lump the whole noise spectrum to one frequency ω_0 so that $M''(q,\omega)$ is proportional to $\delta(\omega - \omega_0)$. The coefficient of proportionality should be compatible with the sum rule

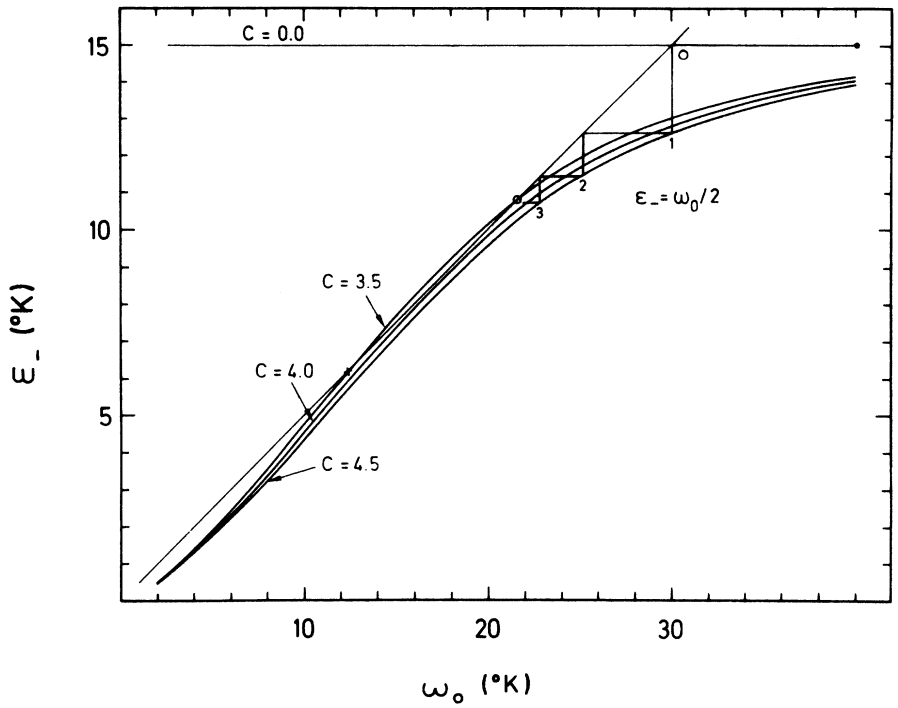

FIG. 11. Graphical solution of the self-consistency equation $\epsilon_-(\omega_0) = \frac{1}{2}\omega_0$ for effective couplings $C = 3.5$, 4.0, and 4.5 in $(10\,°K)^3$.

$$\frac{1}{\pi}\int_0^\infty d\omega\, \omega M''(q,\omega) = \left(\frac{m}{q^2}\right)\sum_{\vec{p}} \varphi(\vec{q},\vec{p})^2 s(p) s(|\vec{q}-\vec{p}|) \tag{B1}$$

following from Eqs. (42a) and (29). So we write

$$M''(\omega) = \pi(C/\omega_0)[\delta(\omega-\omega_0)+\delta(\omega+\omega_0)]. \tag{B2}$$

From Eq. (21) one finds the susceptibility for the model to be

$$\chi(z) = -\left(\frac{q^2}{m}\right)\left(\frac{\alpha}{z^2-\epsilon_-^2}+\frac{1-\alpha}{z^2-\epsilon_+^2}\right), \tag{B3}$$

where

$$2\epsilon_\pm^2 = (\Omega_0^2+\omega_0^2+2C/\omega_0) \pm [(\Omega_0^2-\omega_0^2+2C/\omega_0)^2+8C\omega_0]^{1/2}. \tag{B4}$$

The low resonance ϵ_- represents the elementary excitation while the high resonance ϵ_+ simulates the continuum part. In Fig. 11 the resonance ϵ_- is plotted as a function of ω_0 for $\Omega_0 = 15$ °K and some representative values of C. The numbers for Ω_0 and C roughly reflect the realistic situation for the roton. The resonance ϵ_- is always smaller than Ω_0 and decreases with decreasing ω_0 and increasing C. The spectrum of $M''(q,\omega)$, given by two-mode excitations, is well peaked at twice the energy of the one-mode excitations. Thus one can simulate the crucial self-consistency equations (42) by the requirement

$$\epsilon_-(\omega_0) = \tfrac{1}{2}\omega_0. \tag{B5}$$

Equations (B4) and (B5) then fix ω_0 and ϵ_- as functions of C and Ω_0.

The solution is envisaged most clearly by looking for the intersection of the ϵ_- vs ω_0 curve with the $\omega_0/2$ vs ω_0 line in Fig. 11. There is always the collapse solution $\omega_0 = \epsilon_- = 0$. If the coupling C is larger than a critical value (about 4 in Fig. 11) the collapse solution is the only one. Iteration proceeds via $\epsilon_0, \epsilon_1, \epsilon_2, \ldots$ in steps of almost equal size towards zero. If the coupling C is smaller than the critical value there are two further solutions: a large one (indicated by 0 in Fig. 11) and a small one (indicated by * in Fig. 11). The small one cannot be obtained from ϵ_0 by switching on C continuously; therefore it has no physical meaning. This unphysical solution cannot be obtained by iteration; it is unstable in this respect. The large solution should be considered as the physical one; it can be obtained by iteration, whenever the iteration starts with ϵ_0 above the unstable unphysical solution. If the iteration starts below the unstable solution it yields again the collapse. Taking the self-consistency equation (29) into account lowers ϵ_- but does not change the preceding discussion qualitatively.

One important feature is missing in the model so far. The presence of a continuum part $\chi_c''(q,\omega)$ implies $f(q) < 1$ in Eq. (29). So one has $f < 1$ whenever $\epsilon(q) < \epsilon_0(q)$. Now it is essentially only the 1-1 contribution in Eq. (42b) causing the peak of $M''(q,\omega)$ around 2ϵ. The other terms in $M''(q,\omega)$, in lowest

approximations, can be considered as a constant contribution in $M'(q,\omega)$. Hence one should not consider C as a constant but impose the further self-consistency equation

$$C = C_0 f^2, \tag{B6}$$

where $f = (\alpha/\epsilon_-)/[\alpha/\epsilon_- + (1-\alpha)/\epsilon_+]$ is the strength factor of the model. We do not want to discuss the equation in detail but restrict ourselves to the following reasoning. Possibly C_0 is larger than the critical value, say $C_0 = 4.5$ in the units used in Fig. 11. Then a change of f to 0.88 would be sufficient to yield $C = 3.5$ with a reasonable solution ϵ_-. Iterating the self-consistency equations, however, would probably not yield the solution; in the first step $f_0 = 1$, i.e., a much too large C is used. In the second step f_1 still will be too big, etc. Hence the iteration may pass the unstable solution and run into the collapse.

So the model can exhibit three types of behavior. Case (i): The decay vertex is so small, that there is a physical solution which can be obtained by straightforward iteration starting with $M'' = 0$. This case is not realized for liquid helium as shown in Appendix A. Case (ii): The decay vertex is so big, that there is the collapse solution $\epsilon_- = 0$ only. Then the whole discussion leading to the self-consistency equations loses its basis. Case iii: There is a reasonable solution, but iteration runs into a mathematical instability. In this case, one should find the solution by slowly switching on the vertex, allowing for an appropriate adjustment of the important strength factor f. Case (iii) simulates the liquid-helium situation as is shown in Sec. IV.

---

*Present address: Department of Physics, Harvard University, Cambridge, Mass. 02138.

[1]L. D. Landau, J. Phys. USSR 5, 71 (1941); 11, 91 (1947).
[2]N. N. Bogoliubov, J. Phys. USSR 11, 23 (1947).
[3]T. D. Lee, K. Huang, and C. N. Yang, Phys. Rev. 106, 1135 (1957); S. T. Beliaev, Zh. Eksp. Teor. Fiz. 34, 417 (1958); 34, 433 (1958) [Sov. Phys.—JETP 34, 289; 34, 299 (1958)]; N. Hugenholz and D. Pines, Phys. Rev. 116, 489 (1959).
[4]R. P. Feynman, Phys. Rev. 91, 1291 (1953); 91, 1301 (1953); 94, 262 (1954).
[5]A. Bijl, Physica 7, 869 (1940).
[6]R. P. Feynman, in *Progress in Low Temperature Physics*, edited by C. J. Gorter (North-Holland, Amsterdam, 1955); W. Brenig, Z. Phys. 144, 488 (1956).
[7]R. P. Feynman and M. Cohen, Phys. Rev. 102, 1189 (1956); M. Cohen and R. P. Feynman, Phys. Rev. 107, 13 (1957).
[8]L. P. Pitaevskij, Zh. Eksp. Teor. Fiz. 36, 1168 (1959); 39, 216 (1960) [Sov. Phys.—JETP 9, 830 (1959); 12, 155 (1961)].
[9]C. G. Kuper, Proc. R. Soc. Lond. 233, 223 (1955).
[10]H. W. Jackson and E. Feenberg, Rev. Mod. Phys. 34, 686 (1962).
[11]H. W. Jackson, Phys. Rev. 185, 186 (1969); A 8, 1529 (1973).
[12]W. Götze and M. Lücke, preceding paper, Phys. Rev. B 13, xxxx (1976).
[13]A. Miller, D. Pines, and P. Nozieres, Phys. Rev. 127, 1452 (1962).
[14]K. A. Brueckner and K. Sawada, Phys. Rev. 106, 1117 (1957).
[15]W. E. Parry and D. Ter Haar, Ann. Phys. (N.Y.) 19, 496 (1962).
[16]S. Sunakawa, S. Yamasaki, and T. Kebukawa, Prog. Theor. Phys. 41, 919 (1969); T. Kebukawa, S. Yamasaki, and S. Sunakawa, *ibid.* 44, 565 (1970); 49, 1802 (1973).
[17]J. A. Carballo and J. Ruvalds (unpublished).
[18]J. Ruvalds and A. Zawadowski, Phys. Rev. Lett. 25, 333 (1970); A. Zawadowski, J. Ruvalds, and J. Solana, Phys. Rev. A 5, 399 (1972).
[19]D. K. Lee, Phys. Rev. 162, 134 (1967); H. W. Lai, H. H. Sim, and C. W. Woo, Phys. Rev. A 1, 1536 (1970).
[20]H. Palevsky, K. Otnes, and K. E. Larson, Phys. Rev. 108, 1346 (1957); H. Palevsky, K. Otnes, and K. E. Larson, Phys. Rev. 112, 11 (1958); J. L. Yarnell, G. P. Arnold, P. J. Beadt, and E. C. Kerr, Phys. Rev. 113, 1379 (1959); D. A. Henshaw and A. D. B. Woods, Phys. Rev. 121, 1266 (1961).
[21]R. A. Cowley and A. D. B. Woods, Can. J. Phys. 49, 177 (1971); Rep. Prog. Phys. 36, 1135 (1973).
[22]H. Mori, Prog. Theor. Phys. 33, 423 (1965); 34, 399 (1965).
[23]D. N. Zubarev, Usp. Fiz. Nauk. 71, 71 (1960) [Sov. Phys.-Usp. 3, 320 (1960)]; P. C. Martin, in *Problème à N corps*, edited by C. de Witt and R. Balian (Gordon and Breach, New York, 1968).
[24]L. Van Hove, Phys. Rev. 95, 249 (1954).
[25]E. K. Achter and L. Meyer, Phys. Rev. 188, 291 (1969); R. B. Hallock, Phys. Rev. A 5, 320 (1972).
[26]W. L. McMillan, Phys. Rev. A 138, 442 (1965); W. E. Massey, Phys. Rev. 151, 153 (1966); N. Mihara and R. D. Puff, Phys. Rev. 174, 221 (1968); M. H. Lee, Physica 43, 132 (1969); C. E. Campbell and E. Feenberg, Phys. Rev. 188, 396 (1969); W. P. Francis, G. V. Chester, and L. Reatto, Phys. Rev. A 1, 86 (1970).
[27]G. Gilat and L. J. Raubenheimer, Phys. Rev. 144, 390 (1966).
[28]The curves for $\epsilon(q)$ published in Ref. 10 and 11 are not in agreement with each other. The discrepancy has not been explained but possibly it is due to different structure factors $s(q)$ being used. We show here and in the following the results of Ref. 11, since they agree with our own numerical results (Ref. 12) of the Jackson-Feenberg theory.